Electronic Supplementary Material (ESI) for ChemComm.

Electronic Supplemental Information

Hydrogen release reactions of Al-based complex hydrides enhanced by vibrational dynamics and valences of metal cations

T. Sato,[a] A. J. Ramirez–Cuesta,[b] L. Daemen,[b] Y. –Q. Cheng,[b] K. Tomiyasu,[c] S. Takagi,[a] and S. Orimo*[a, d]

[a.] Institute for Materials Research, Tohoku University, Aoba, Sendai 980-8577, Japan

[b.] Chemical and Engineering Materials Division, Neutron Sciences Directorate, ORNL, 1 Bathel Valley Road, Oak Ridge, Tennessee 37831, USA

[c.] Department of Physics, Tohoku University, Aoba, Sendai 980-8578, Japan

[d.] WPI-Advanced Institute for Materials Research, Tohoku University, Aoba, Sendai 980-8577, Japan.

Table of Contents

1. Methods

Sample preparations. $LiAlH_4$ was purchased from Simga–Aldrich, (95%). $Ca(AlH_4)_2$ was directly synthesized by mechanochemical milling of CaH_2 and AlH_3 in a molar ratios of 1:2. CaH_2 as the starting material was yielded from hydrogenation of dendritic pieces of Ca (Sigma–Aldrich, 99.99%) at 673 K in a hydrogen gas pressure of 0.5 MPa for 10h. AlH_3 as the starting material was synthesized in diethyl ether according to the chemical reaction of $LiAlH_4$ and $AlCl_3$.[S1] The mixture was milled at 400 r.p.m. under a hydrogen gas pressure of 0.2 MPa using Fritsch P7. $LiCa(AlH_4)_3$ was directly synthesized by mechanochemical milling of LiH (Alfa Aesar, 99.4%), CaH_2 and AlH_3 in a molar ratios of 1:1:3. The mixture was milled at 400 r.p.m. under a hydrogen gas pressure of 0.2 MPa using Fritsch P7. The effective milling time to obtain $Ca(AlH_4)_2$ and $LiCa(AlH_4)_3$ was 10 hours.[S2, S3] Milling time of 15 min was alternated with pauses of 5 min duration. All samples were handled in Ar or He gas filled glove boxes with a dew point below 183 K and with less than 1 ppm of O_2 to prevent (hydro-) oxidation.

X-ray diffraction. All samples were investigated by using a powder X-ray diffractometer (PANalytical X'PERT, with Cu Kα radiation (wavelength λ = 1.5406 Å for Kα1 and 1.5444 Å for Kα2)). The samples were covered by a Kapton tape in order to prevent (hydro-) oxidation during the measurement. In order to prevent (hydro-) oxidation during X-ray diffraction measurement, the sample was covered with a Kapton tape.

Raman and Fourier Transform Infrared (FTIR) spectroscopies. The Raman spectra of all samples were obtained by Nicolet Almega-HD with a Nd:YVO_4 laser (532 nm). The samples were placed under Ar gas in a sample holder with a glass window, and spectra were measured using the backscattering configuration with a microscope Raman spectrometer. The FTIR spectra of all samples were obtained by Thermo Scientific Nicolet iZ10. A thin sample, approximately a few μm thick, was prepared in an Ar-gas-filled diamond anvil cell, and transmission spectra were measured with a microscope FTIR spectrometer.

Inelastic neutron scattering (INS). The samples (approximately 1.0 g) were sealed in an airtight Al container. The INS spectra of all samples were obtained at 10–400 K for 1 h. At 400 K, the temperature kept for 3 h. The INS spectra were obtained by an inverted geometry INS spectrometer, VISION, with high resolution (1.5% ΔE/E) and broader frequency range (–15–8000 cm^{-1}) at the Spallation Neutron Source SNS, Oak Ridge National Laboratory in USA.

Computational.

Density function theory (DFT) calculations were performed using CASTEP.[S4] The Generalized Gradient Approximation (GGA), as implemented by Perdew-Burke-Ernzerhof (PBE), was used to describe the exchange-correlation interactions. Norm-conserving pseudopotentials were employed to account for the effects of core electrons. The unit cell configurations were obtained (from literature or from your own XRD data), and the atomic coordinates were relaxed under the constraints of the symmetry. The energy tolerance for the electronic structure calculations was $5x10^{-10}$ eV, and the energy tolerance for ionic relaxation was $5x10^{-9}$ eV. The tolerance for the interatomic forces was 0.001 eV/Å. After convergence was reached, the force constants and the dynamical matrix were obtained using the density functional perturbation theory, from which the phonon frequencies and vibrational modes were calculated. The electronic structure calculations were performed on a 4x3x3 Monkhorst-Pack mesh, and the phonon calculations were performed on a 4x3x3 gamma-centered grid in the Brillouin zone, interpolated on a 12x6x6 grid for the density of states and INS calculation. The aCLIMAX software[S5] was used to convert the DFT-calculated phonon results to the simulated INS spectra. Phonon frequencies calculated from DFT with harmonic approximation were slightly scaled by up to 6% in the aCLIMAX software in order to compare with experimental INS spectra observed at 10 K with less thermal vibration and better align/assign the peaks. The scaling did not change the order of the frequencies.

2. Figures

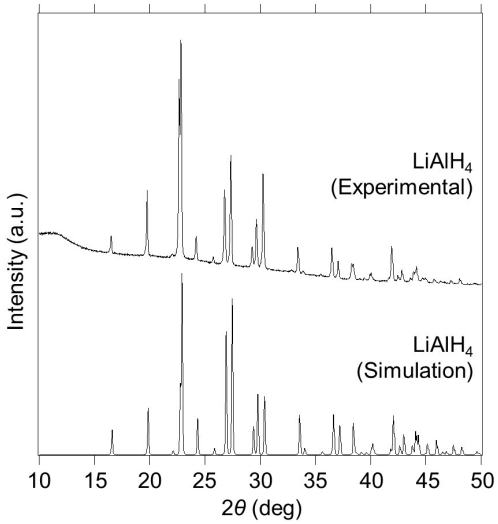

Figure S1 (Top) Experimental and (bottom) simulation X-ray diffraction patterns of $LiAlH_4$. The simulated x-ray diffraction pattern was obtained based on a crystal structure of $LiAlD_4$[S6]. The slope background is due to a Kapton tape.

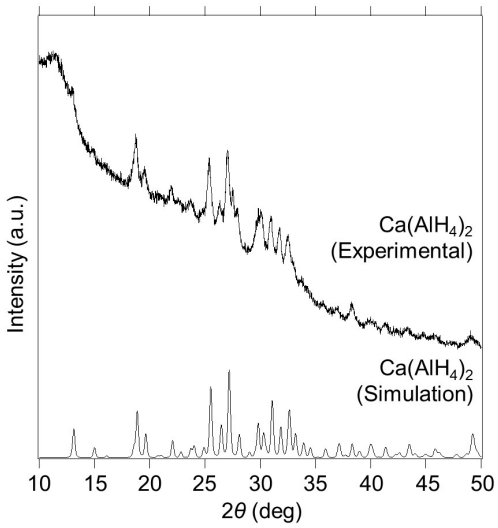

Figure S2 (Top) Experimental and (bottom) simulation X-ray diffraction patterns of $Ca(AlH_4)_2$. The simulated x-ray diffraction pattern was obtained based on a crystal structure of $Ca(AlD_4)_2$[S7]. The slope background is due to a Kapton tape.

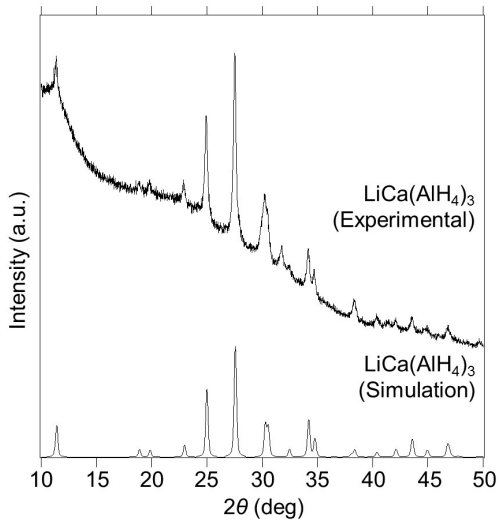

Figure S3 (Top) Experimental and (bottom) simulation X-ray diffraction patterns of $LiCa(AlH_4)_3$. The simulated x-ray diffraction pattern was obtained based on a crystal structure of $LiCa(AlH_4)_3$[S3]. The slope background is due to a Kapton tape.

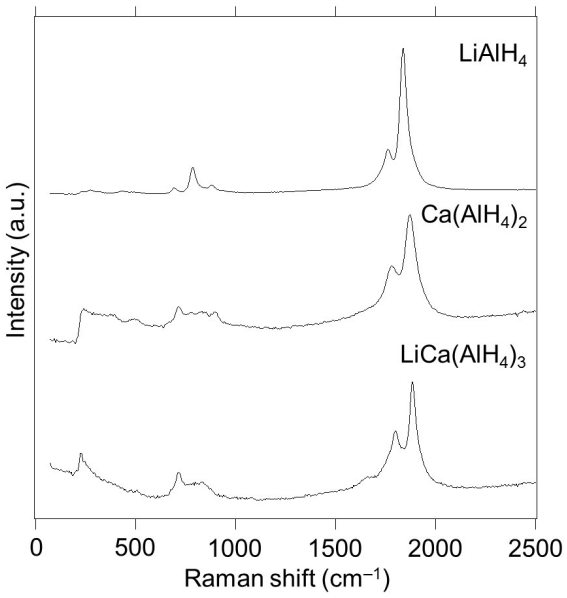

Figure S4 Raman spectra of (top) $LiAlH_4$, (middle) $Ca(AlH_4)_2$ and (bottom) $LiCa(AlH_4)_3$. The peaks at 600–1000 cm^{-1} and 1600–2000 cm^{-1} are assigned to Al–H bending and stretching modes, respectively.

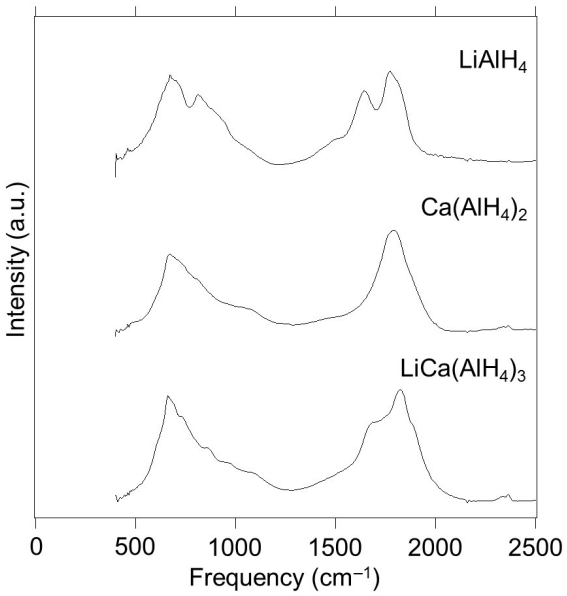

Figure S5 FTIR spectra of (top) $LiAlH_4$, (middle) $Ca(AlH_4)_2$ and (bottom) $LiCa(AlH_4)_3$. The peaks at 600–1200 cm^{-1} and 1500–2000 cm^{-1} are assigned to Al–H bending and stretching modes, respectively.

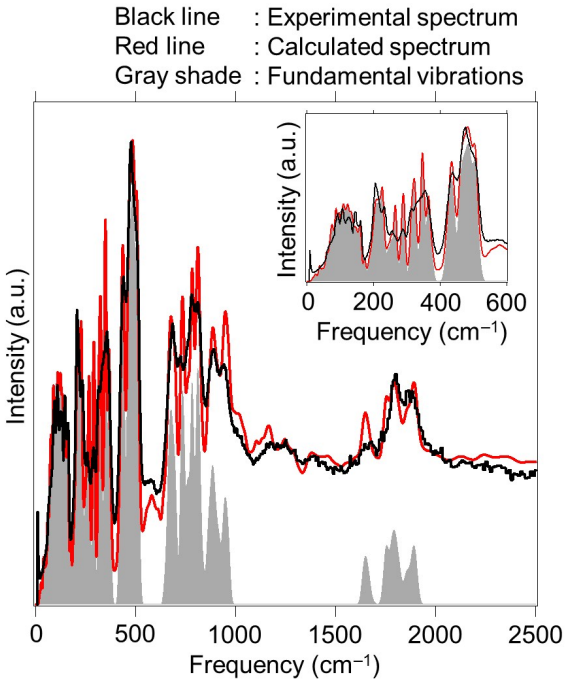

Figure S6 The experimental (black line) and total calculated (red line) INS spectra of $LiAlH_4$. The shaded gray color represents the contribution from the fundamental vibrations. The insert show low frequency region below 600 cm^{-1}

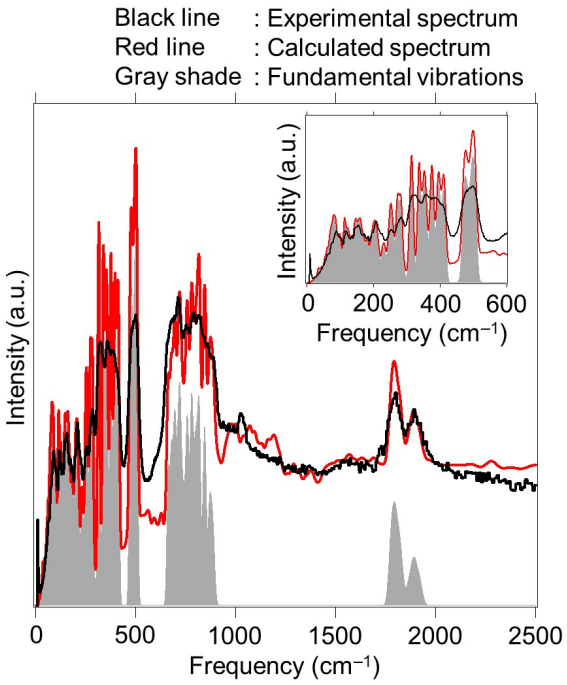

Figure S7 The experimental (black line) and total calculated (red line) INS spectra of $Ca(AlH_4)_2$. The shaded gray color represents the contribution from the fundamental vibrations. The insert show low frequency region below 600 cm^{-1}

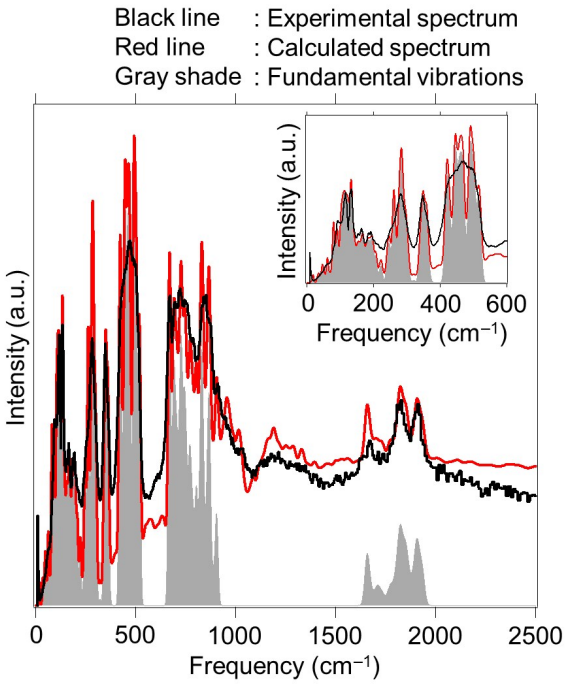

Figure S8 The experimental (black line) and total calculated (red line) INS spectra of $LiCa(AlH_4)_3$. The shaded gray color represents the contribution from the fundamental vibrations. The insert show low frequency region below 600 cm^{-1}

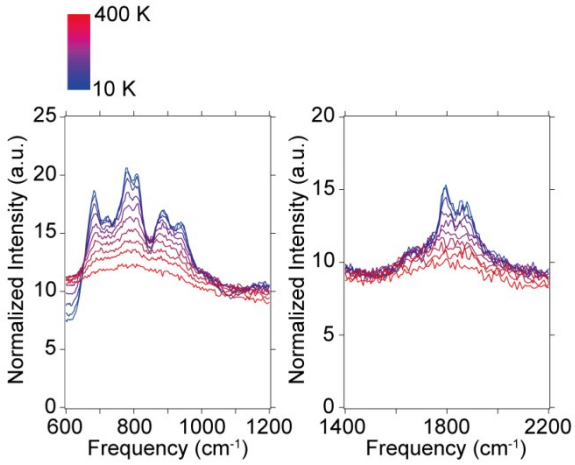

Figure S9 INS spectra of $LiAlH_4$ at the frequency range of (left) 600–1200 cm^{-1} and (right) 1400–2200 cm^{-1} at 10 – 400 K. The intensity was are divided by the Bose factor, $B(E, T) = 1 + 1/[\exp\{E/k_BT\} - 1]$.[S8] In the Bose factor, E: energy transfer in meV (= 8.066 × Frequency in cm^{-1}), T: Temperature in kelvin and k_B: Bolzmann constant in J/K.

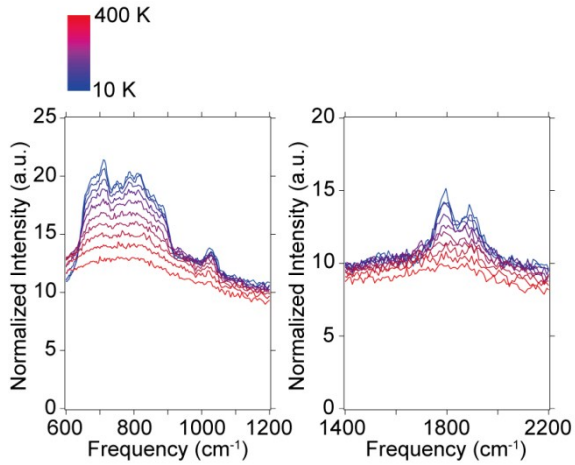

Figure S10 INS spectra of $Ca(AlH_4)_2$ at the frequency range of (left) 600–1200 cm^{-1} and (right) 1400–2200 cm^{-1} at 10 – 400 K. The intensity was are divided by the Bose factor, $B(E, T) = 1 + 1/[\exp\{E/k_BT\} - 1]$.[S8] In the Bose factor, E: energy transfer in meV (= 8.066 × Frequency in cm^{-1}), T: Temperature in kelvin and k_B: Bolzmann constant in J/K.

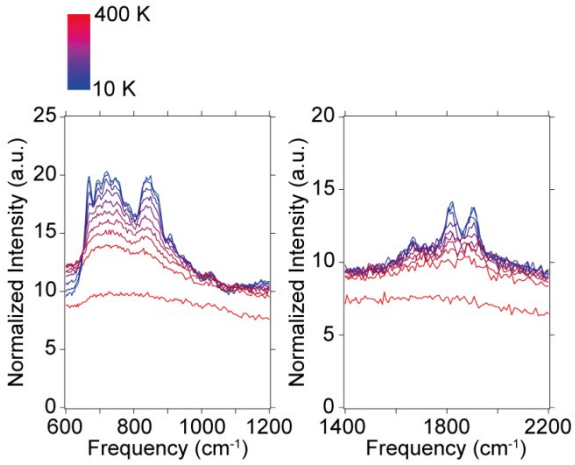

Figure S11 INS spectra of $LiCa(AlH_4)_3$ at the frequency range of (left) 600–1200 cm^{-1} and (right) 1400–2200 cm^{-1} at 10 – 400 K. The intensity was are divided by the Bose factor, $B(E, T) = 1 + 1/[\exp\{E/k_BT\} - 1]$.[S8] In the Bose factor, E: energy transfer in meV (= 8.066 × Frequency in cm^{-1}), T: Temperature in kelvin and k_B: Bolzmann constant in J/K.

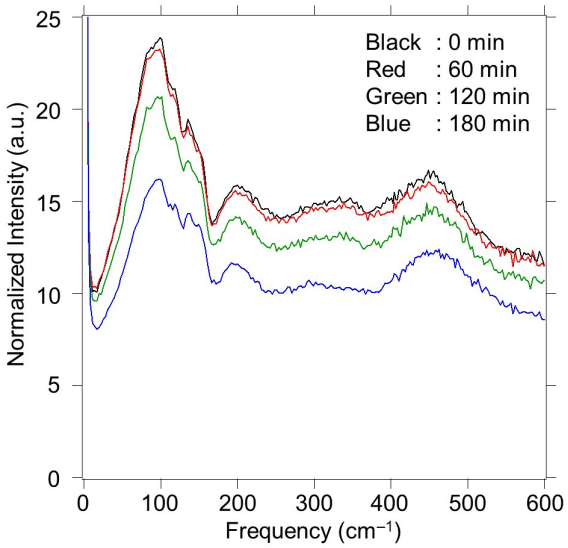

Figure S12 INS spectra of $LiAlH_4$ at the frequency region of 0–600 cm^{-1} at 400 K for 0 – 180 min. Black, red, green and blue lines are obtained at 0, 60, 120 and 180 min, respectively, after reaching at 400 K. Each spectrum was collected for 15 min. The intensity was are divided by the Bose factor, $B(E, T) = 1 + 1/[\exp\{E/k_BT\} - 1]$.[S8] In the Bose factor, E: energy transfer in meV (= 8.066 × Frequency in cm^{-1}), T: Temperature in kelvin and k_B: Bolzmann constant in J/K.

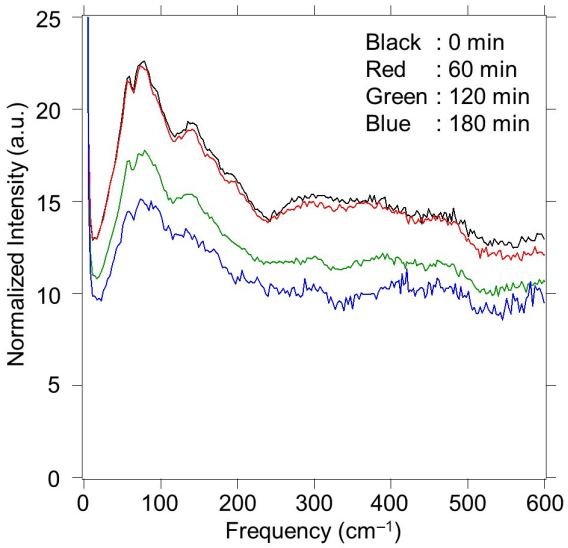

Figure S13 INS spectra of $Ca(AlH_4)_2$ at the frequency region of 0–600 cm^{-1} at 400 K for 0 – 180 min. Black, red, green and blue lines are obtained at 0, 60, 120 and 180 min, respectively, after reaching at 400 K. Each spectrum was collected for 15 min. The intensity was are divided by the Bose factor, $B(E, T) = 1 + 1/[\exp\{E/k_BT\} - 1]$.[S8] In the Bose factor, E: energy transfer in meV (= 8.066 × Frequency in cm^{-1}), T: Temperature in kelvin and k_B: Bolzmann constant in J/K.

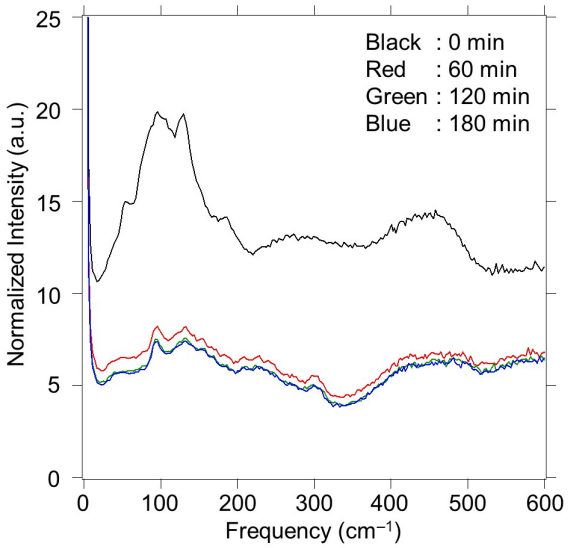

Figure S14 INS spectra of $LiCa(AlH_4)_3$ at the frequency region of 0–600 cm^{-1} at 400 K for 0 – 180 min. Black, red, green and blue lines are obtained at 0, 60, 120 and 180 min, respectively, after reaching at 400 K. Each spectrum was collected for 15 min. The intensity was are divided by the Bose factor, $B(E, T) = 1 + 1/[\exp\{E/k_BT\} - 1]$.[S8] In the Bose factor, E: energy transfer in meV (= 8.066 × Frequency in cm^{-1}), T: Temperature in kelvin and k_B: Bolzmann constant in J/K.

References

S1 (a) F. M. Brower, N. E. Matzek, P. F. Riegler, H. W. Rinn, C. B. Roberts, D. L. Schmidt, J. A. Snover and K. Terada, *J. Am. Chem. Soc.,* 1976, **98**, 2450; (b) K. Ikeda, S. Muto, K. Tatsumi, M. Menjo, S. Kato, M. Bielmann, A. Züttel, C. M. Jensen, and S. Orimo, *Nanotechnology*, 2009, **20**, 204004.

S2 T. Sato, K. Ikeda, H.-W. Li, H. Yukawa, M. Morinaga and S. Orimo, *Mater. Trans.*, 2009, **50**, 182 – 186.

S3 T. Sato, S. Takagi, S. Deledda, B. C. Hauback and S. Orimo, *Sci. Rep.*, 2016, **6**, 23592.

S4 S.J. Clark, M.D. Segall, C.J. Pickard, P.J. Hasnip, M.J. Probert, K. Refson and M.C. Payne, *Z. Kristallogr.,* 2005, **220**, 567 – 570.

S5 A.J. Ramirez-Cuesta, *Comput. Phys. Commun.,* 2004, **157**, 226 – 238.

S6 B. C. Hauback, *Z, Kristallogr.*, 2008, **223**, 636 – 648.

S7 T. Sato, M. H. Sørby, K. Ikeda, S. Sato, B. C. Hauback and S. Orimo, *J. Alloys Compd.*, 2009, **487**, 472 – 478.

S8 Q. Shi, J. Voss, H.S. Jacobsen, K. Lefmann, M. Zamponi and T. Vegge, *J. Alloys Compd.*, 2007, **446 – 447**, 469 – 473.